Carrier capture into a GaAs quantum well with a separate confinement region: comment on quantum and classical aspects

Martin Moško and Karol Kálna

Institute of Electrical Engineering, Slovak Academy of Sciences, Dúbravská cesta 9, 842 39 Bratislava, Slovakia

Abstract. We study the optic-phonon-mediated carrier capture in a narrow GaAs quantum well with a 100 nm separate confinement region. In a standard quantum model capture means the carrier scattering from the energy subband above the quantum well into a subband in the quantum well. We use the quantum model in parallel with a classical model in which a classical carrier is captured during collisionless motion when emitting the optic phonon inside the GaAs layer. Comparison with the experiment of Blom *et al* (1993 *Phys. Rev.* B **47** 2072) suggests that the quantum capture model is valid not only for electrons but also for heavy holes in the case of very narrow (2.6 nm) quantum wells. In the case of wider quantum wells the available experimental data support equally the quantum as well as classical hole capture models and do not allow us to draw a definite conclusion. Finally, the effect of the phonon confinement on the quantum capture is evaluated and discussed.

1. Introduction

Carrier capture into a quantum well is an important transport process in semiconductor quantum well lasers [1, 2] and a subject of time-resolved optical studies [3–6]. To model the capture process in a laser device or in a time-resolved experiment, it is in general necessary to consider the capture of electrons and holes via the carrier–optic phonon [7] and carrier–carrier [8] scattering. The latter process is important at high carrier densities [8]; the optic-phonon-mediated capture is important in any case and certainly dominates at low densities.

A standard theory of the optic-phonon-mediated capture relies on a so-called quantum capture model in which the capture is essentially the carrier scattering from the energy subband above the quantum well to the energy subband in the quantum well, with the scattering probability described by the Fermi golden rule. Figure 1 shows the subband levels in a separate confinement heterostructure quantum well used in the capture time measurements of [6]. The quantum capture model predicts that the electron capture time oscillates as a function of the quantum well width, which seems to be confirmed experimentally [6].

However, since the quantum capture model assumes a well defined subband structure (figure 1) with coherent envelope functions, it is expected to fail when the carrier coherence length is smaller than the width of the AlGaAs/GaAs/AlGaAs region. Then, the classical capture model, in which the carriers move across the AlGaAs barriers
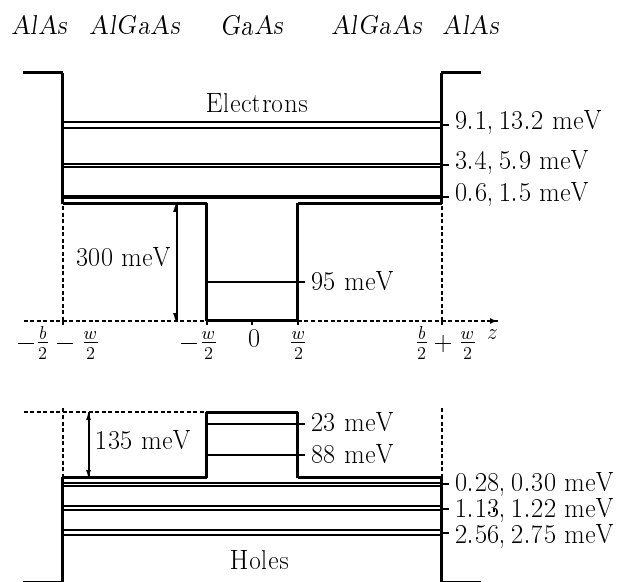

Figure 1. Energy band profile of the separate confinement heterostructure quantum well consisting of the GaAs quantum well between two $Al_{0.3}Ga_{0.7}As$ barriers and two thick AlAs cladding layers. The structure is undoped. The thickness of the AlGaAs barrier is $b/2 = 50$ nm; the energy subbands of electrons and heavy holes are shown for a 4.3 nm quantum well.

classically, is considered to be a better alternative [1, 6]. To interpret their experimental results, Blom *et al* [6] assumed

that the capture in the structure of figure 1 is of quantum nature for electrons and of classical nature for (heavy) holes, with the hole capture time given by the diffusion time through the AlGaAs barrier.

This paper provides a rather different interpretation. In accord with Blom *et al* [6], also our results support the validity of the quantum capture model for electrons. However, we find that the experiment indicates also the presence of the quantum hole capture in case of very narrow (2.6 nm) quantum wells, while for wider quantum wells the available experimental data support equally the quantum as well as classical hole capture models. It is also proposed that the hole dynamics in the classical capture model is not a diffusion process but a collisionless motion combined with the phonon emission in the GaAs layer. Finally, the quantum capture model is shown to be affected by the phonon confinement.

In section 2 we discuss the quantum capture model, in section 3 the classical one. Comparison with experiment is given in section 4 and the appendix summarizes the formulae describing the phonon confinement.

2. Quantum capture model

We consider the electron and heavy-hole states in the structure of figure 1 within the usual effective mass approximation, with the material parameters properly interpolated between GaAs and AlAs [9]. For $x = 0.305$ we have a 0.3 eV quantum well (QW) depth for electrons (the same QW depth was assumed in the experiment of interest [6]) and a 0.13 eV QW depth for heavy holes. In what follows we label the energy and the envelope function of subband i as E_i and $\chi_i(z)$, respectively. Let a carrier be initially in the subband i and let the kinetic energy of the carrier free motion (the motion parallel with the heterointerface) be ε. The scattering rate from subband i to subband j, $\lambda_{ij}(\varepsilon)$, is a simple expression, if one assumes the scattering by bulk (GaAs-like) polar LO phonons. A standard Fermi golden rule based calculation then gives [10]

$$\lambda_{ij}(\varepsilon) = \frac{e^2 \omega_L m}{8\pi\hbar^2}\left(\frac{1}{\kappa_\infty} - \frac{1}{\kappa_S}\right)\int_0^{2\pi} d\theta \frac{F_{iijj}(q)}{q} \quad (1)$$

$$q = \frac{\sqrt{2m}}{\hbar}[2\varepsilon - E - 2\varepsilon^{1/2}(\varepsilon + E)^{1/2}\cos\theta]^{1/2} \quad (2)$$

$$F_{iijj}(q) = \int_{-\infty}^{\infty} dz \int_{-\infty}^{\infty} dz' \, \chi_i(z)\chi_i(z') e^{-q|z-z'|}\chi_j(z)\chi_j(z') \quad (3)$$

and $E = \varepsilon - E_j + E_i - \hbar\omega_L$. Here m is the carrier effective mass, ω_L is the LO phonon frequency, κ_S the static permittivity and κ_∞ the dynamic permittivity, all related to the GaAs material. Note that in equation (1) only the spontaneous emission of phonons is included since the temperature in the experiment [6] is only 8 K.

Once we know $\lambda_{ij}(\varepsilon)$, the carrier capture time (τ) can be evaluated as a reciprocal of the mean capture rate

$$\frac{1}{\tau} = \sum_{i,j,\varepsilon} f_i(\varepsilon)\lambda_{ij}(\varepsilon)\left(\sum_{i,\varepsilon} f_i(\varepsilon)\right)^{-1} \quad (4)$$

where the summation over i (j) includes the carrier subbands above (below) the AlGaAs barrier and $f_i(\varepsilon)$ is the carrier distribution.

Equation (1) is a bulk phonon approximation, which ignores the phonon confinement resulting from the presence of various materials. The effect of the phonon confinement [11, 12] has not been so far considered in the structure of figure 1 and the capture time data from that structure were interpreted in the bulk phonon approximation [6]. Here we consider the phonon confinement within the dielectric continuum (DC) model [13, 14] which distinguishes the confined and interface phonon modes. The DC model seems to fit well the microscopic theory [15, 16] and has already been applied in the capture rate calculations [17, 18]. Scattering rate expressions for the DC model are given in the literature [13, 15]; we accommodate them for the structure of interest in the appendix, where we give the scattering rates for the confined as well as interface phonon modes. Inserting the sum of these rates for $\lambda_{ij}(\varepsilon)$ in equation (4) we obtain the capture time expression which incorporates the effect of both confined and interface phonons.

Now we determine the carrier distribution $f_i(\varepsilon)$ by following the authors of [6]. In their experiment electrons and holes are excited above the AlGaAs barrier by a short (1 ps) quasi-monoenergetic laser pulse. The matrix element describing the optical transition from the valence subband l to the conduction subband i is proportional [19, 20] to the overlap integral $\int_{-\infty}^{\infty} dz \, \chi_i^e(z)\chi_l^h(z)$, which is close to unity for $i = l$ and close to zero for $i \neq l$. This implies that the same number of electron and hole subbands is occupied after the excitation and that each carrier subband is occupied by the same number of carriers. Thus, the photoexcited distributions are

$$f_i^e(\varepsilon) \approx C\,\delta(\varepsilon - G_i^e) \qquad f_i^h(\varepsilon) \approx C\,\delta(\varepsilon - G_i^h) \quad (5)$$

where C is the normalization constant and G_i^e and G_i^h are the electron and hole excitation energies in the ith subband ($G_i^e = m_h(E_{ex} - E_i^e - E_i^h)/(m_e + m_h)$ and $G_i^h = m_e(E_{ex} - E_i^e - E_i^h)/(m_e + m_h)$, where E_{ex} is the laser excess energy). We assume $E_{ex} = 36$ meV [6] in numerical calculations.

In figure 2 the quantum capture time is evaluated by using the bulk phonon model (1) as well as by using the DC phonon model from the appendix. One sees that in the case of electrons the results of the DC phonon model exceed the results of the bulk phonon model roughly by a factor of one to three. This difference deserves a more detailed discussion as it contradicts the expectation (see p 2078 in [6]) according to which the incorporation of the phonon two dimensionality should have only a negligible effect on the capture process described by assuming bulk phonons. The authors of [6] pointed out that the overlap of the wavefunction of the electron barrier state (initial state) with the wavefunction of the electron bound state (final state) is significantly larger inside the barrier layers than inside the QW layer and they correctly argued that a major contribution to the scattering rate comes from the phonons inside the barrier layers. Since the barrier layers are bulklike, the expectation [6] that the capture process is well described by assuming bulk phonons seems to be justified. We wish to point out that these considerations overlook the following important issue.
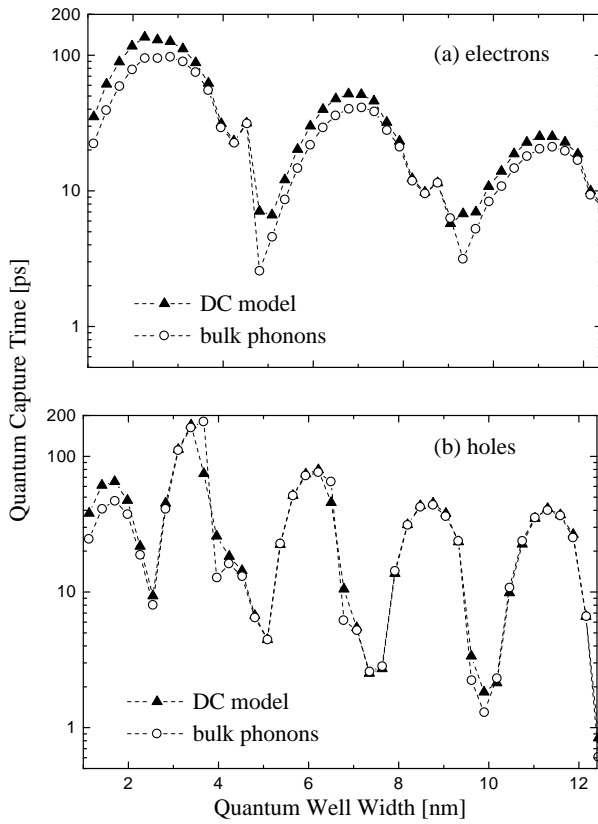
Figure 2. Quantum capture time as a function of the QW width for electrons and heavy holes. The QW widths used in the calculations are integer multiples of the crystal monolayer width.

The wavefunction of the confined phonon modes in the DC model is zero at the AlGaAs/GaAs interface (and therefore strongly suppressed in the vicinity of the interface) whereas the bulk phonon wavefunction is not. Additionally, the wavefunction overlap of the initial (barrier) and final (bound) electron states is only significant in the vicinity of the AlGaAs/GaAs interface due to the exponential decay of the bound wavefunction. Therefore, the scattering via the confined phonon modes is inherently weaker than the scattering via the bulk phonon modes and does not approach the latter even in case of the bulklike barrier layers. As a result, the DC model based capture time exceeds the bulk model based capture time (figure 2). On the other hand, the interface phonon modes are exponentially localized near the interface and the scattering by these modes tends to compensate the suppression of the confined phonon mode scattering. As a result, the DC model based capture time also depends on the level of this compensation and, in principle, can become even smaller than the bulk model based capture time (this is what we see in figure 2(b) in some cases).

It is worth mentioning that if we insert into our scattering rate formulae just the wavefunction of the lowest bound state, we recover the well known [15] results for the intrasubband scattering rate $\lambda_{11}(\varepsilon)$ in the lowest subband of the GaAs QW (see figure 3). This simple situation is easy to understand: at small QW widths the $\lambda_{11}(\varepsilon)$ from the DC phonon model exceeds the $\lambda_{11}(\varepsilon)$ from the bulk phonon model due to the dominant role of the interface modes; at large QW widths the
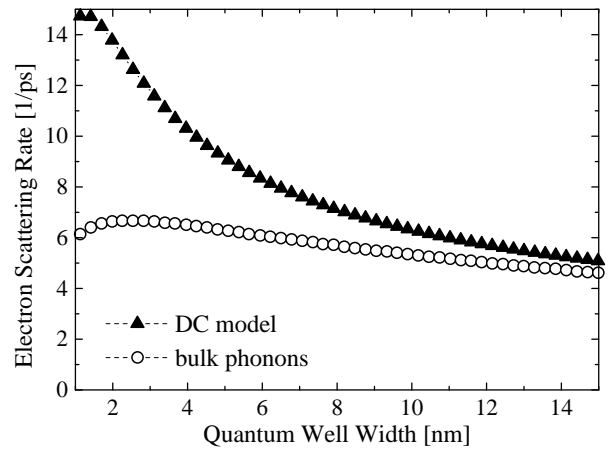
Figure 3. Electron scattering rate in the lowest QW subband, $\lambda_{11}(\varepsilon)$, as a function of the QW width for $\varepsilon = 100$ meV.

effect of the interface modes becomes weak and the effect of the confined modes approaches the bulk phonon effect.

3. Classical capture model

In [6] the classical capture time of holes was determined as a diffusion time through the AlGaAs barrier,

$$\tau = (b/2)^2/(2D) \tag{6}$$

where D is the diffusion constant. D was determined from the hole mobility (μ_h) in doped AlGaAs bulk samples and the resulting hole capture time was $\tau = 12.5$ ps [6], which corresponds to $D = 1$ cm^2 s^{-1} and $\mu_h = 1440$ cm^2 V^{-1} s^{-1}. Let us examine the applicability of these estimates.

Since $\mu_h = 1440$ cm^2 V^{-1} s^{-1} is the hole mobility in the doped AlGaAs, we believe that it strongly underestimates the actual hole mobility in the undoped AlGaAs barriers. It is known that in undoped GaAs layers the hole mobility is as high as 20 000 cm^2 V^{-1} s^{-1} at 10 K and 54 000 cm^2 V^{-1} s^{-1} at 4.2 K ([21], pp 391, 394). In the undoped Al$_{0.3}$Ga$_{0.7}$As layer at 8 K the hole mobility should be similar, perhaps slightly reduced by the alloy scattering but still one order of magnitude higher than 1440 cm^2 V^{-1} s^{-1}. For μ_h of the order of 10 000 cm^2 V^{-1} s^{-1} we estimate the hole mean free path ℓ to be several times larger than the width of the AlGaAs barrier ($b/2 = 50$ nm). This invalidates the diffusion concept (6) which is valid only for $\ell \ll b/2$, and also suggests that the hole motion in the AlGaAs barriers is essentially collisionless. A further important aspect not involved in equation (6) is the fact that the classical carrier can cross the GaAs QW without being captured, if the QW width is smaller than the optic-phonon-limited mean free path [22]. Below we present a simple microscopic theory which includes these aspects.

Under the collision-free conditions the hole transit time across the AlGaAs barrier is given by

$$\tau_t = \frac{b/2}{[2G^h/(\pi m)]^{1/2}} \tag{7}$$

where G^h is the hole excitation energy in the AlGaAs barrier (equation (7) is the Bethe formula [22] written for a flat band

structure). Let us write the capture rate as

$$\frac{1}{\tau} = \frac{1}{\tau_t}(1 - e^{-w/\ell_{\rm ph}}). \tag{8}$$

The factor $1 - \exp(-w/\ell_{\rm ph})$ represents the probability that the carrier emits a phonon when moving classically across the GaAs layer, i.e. $\ell_{\rm ph}$ is the optic-phonon-emission-limited mean free path taken for the bulk GaAs. We express $\ell_{\rm ph}$ as $\ell_{\rm ph} = v_h \tau_h$, where v_h is the z-component of the hole velocity after the injection into the QW and $1/\tau_h$ is the optic phonon emission rate evaluated as in the bulk GaAs. For polar phonons [23]

$$\frac{1}{\tau_h(\varepsilon)} = \sqrt{\frac{m}{2}} \frac{e^2 \omega_L}{4\pi\hbar} \left(\frac{1}{\kappa_\infty} - \frac{1}{\kappa_S}\right) \frac{1}{\sqrt{\varepsilon}} \ln\left|\frac{\sqrt{\varepsilon} + \sqrt{\varepsilon - \hbar\omega_L}}{\sqrt{\varepsilon} - \sqrt{\varepsilon - \hbar\omega_L}}\right| \tag{9}$$

where ε is now the carrier kinetic energy after the injection into the QW. The holes also undergo the nonpolar optic phonon scattering via the emission rate [24]

$$\frac{1}{\tau_h(\varepsilon)} = \frac{(2m)^{3/2}D_0^2}{4\pi\hbar^3\rho\omega_0}\sqrt{\varepsilon - \hbar\omega_0} \tag{10}$$

where D_0 is the deformation potential of the nonpolar interaction, ρ is the mass density, v_L is the velocity of sound and ω_0 is the nonpolar optic phonon frequency (values of these parameters are given in [25]).

Finally, the classical capture model (8) can further be improved if we take into account the possibility of quantum reflection (transmission) at the GaAs/AlGaAs heterointerface. This modifies equation (8) as

$$\frac{1}{\tau} = \frac{1}{\tau_t} T_{B\to W}\left[1 - \exp\left(-\frac{w}{v_h\tau_h T_{W\to B}}\right)\right] \tag{11}$$

where $T_{B\to W}$ is the carrier transmission probability at the heterointerface when the carrier passes from the barrier layer (B) into the well layer (W), and $T_{W\to B}$ is the same for the motion from the well layer into the barrier layer. For the heterointerface modelled by a rectangular potential step (figure 1), $T_{B\to W}$ and $T_{W\to B}$ are given by the known textbook formulae [26]. In conditions considered by us the coefficients $T_{B\to W}$ and $T_{W\to B}$ cause only a small (about 10%) reduction of the capture rate.

In figure 4 the classical hole capture time (11) is presented together with the 12.5 ps time constant of [6].

4. Comparison with experiment and discussion

In [6] experimental data were extracted in terms of the ambipolar capture time, which is defined as

$$\frac{1}{\tau_{\rm amb}} = \frac{1}{2}\left(\frac{1}{\tau^{\rm electron}} + \frac{1}{\tau^{\rm hole}}\right) \tag{12}$$

where $\tau^{\rm electron}$ and $\tau^{\rm hole}$ are the electron and hole capture times in a flat band model. Equation (12) roughly incorporates the fact that the space charge effects tend to equalize the electron and hole capture rates so that the actual carrier capture rate is their average [6].
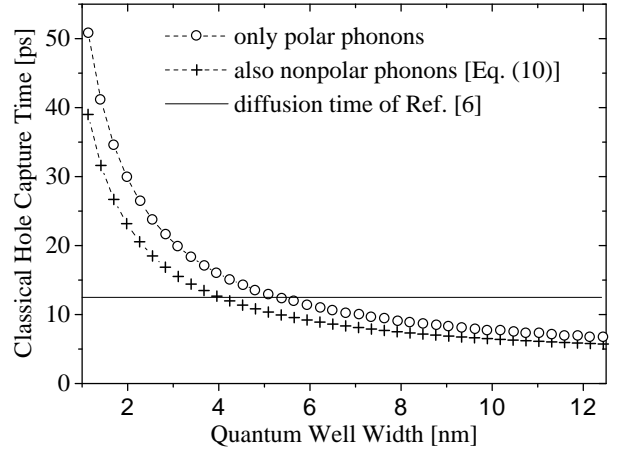

Figure 4. Classical hole capture time as a function of the QW width.
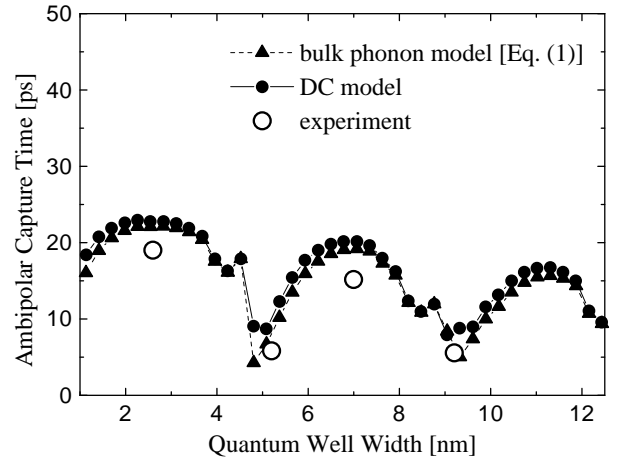

Figure 5. Ambipolar capture time (equation (12)) for two different quantum models of electron capture, the bulk phonon model and the DC model. The capture of holes is assumed to be classical, with $\tau^{\rm hole} = 12.5$ ps. Experimental data of [6] are also shown.

We start by reproducing the calculation of [6] in which $\tau^{\rm hole}$ is the classical diffusive capture time (12.5 ps) and $\tau^{\rm electron}$ is given by the quantum capture model with bulk polar optic phonons (equation (1)). The resulting ambipolar capture time is shown in figure 5 by full triangles. It fits reasonably well the experimental data (open circles) from four QW samples with different QW widths, which were interpreted in [6] as proof for the oscillating electron capture time. However, in the light of the discussion of section 3, the fit should not be viewed as a proof that the hole capture is governed by the diffusion concept (6). In fact, for a more realistic mobility estimate, say for $\mu_h = 10\,000$ cm^2 V^{-1} s^{-1}, equation (6) gives a much smaller τ than 12.5 ps and the fit no longer exists [27]. In other words, the fit with $\tau^{\rm hole} = 12.5$ ps should be viewed as an empirical fit, not as a microscopic interpretation of the hole capture.

Figure 5 also shows the results (full circles) obtained with $\tau^{\rm electron}$ calculated from the DC phonon model. One sees that the effect of the DC phonon model is not negligible, but the fit of experimental data is deteriorated. This is a further motivation to refine the modelling of $\tau^{\rm hole}$. Thus, in
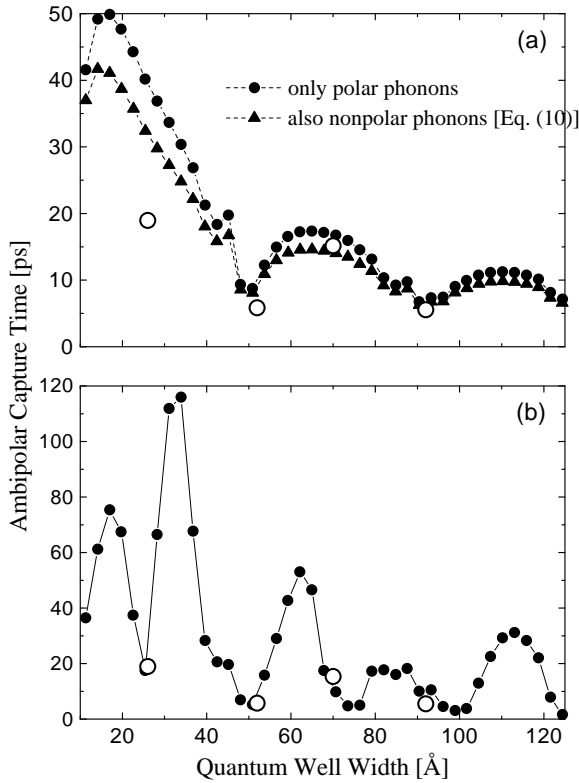
Figure 6. Ambipolar capture time (equation (12)) as a function of the QW width. Figure (a) shows the calculation which involves the classical hole capture according to equation (11) and the quantum electron capture within the DC phonon model. Figure (b) shows the calculation based on the quantum hole capture and quantum electron capture, both treated within the DC phonon model. Experimental data of [6] are shown by open circles.

what follows we keep the DC model for the quantum electron capture and speculate only about the τ^{hole} modelling.

First we calculate τ_{amb} for τ^{hole} given by equation (11). Results are shown in figure 6(a) by full circles and by full triangles (in the former case the holes are scattered only by polar phonons (equation (9)), in the latter case also by nonpolar phonons (equation (10))). The agreement with experiment is quite good at QW widths of 5, 7 and 9 nm; however, at the QW width of 2.6 nm the theory significantly overestimates the measured value. The overestimation is due to the exponential factor in the formula (11), or in other words, owing to $\ell_{\text{ph}} \gg w$ there is a high probability that the classically moving hole crosses the GaAs layer without emitting a phonon. Finally, we calculate τ_{amb} by using the DC phonon model of quantum capture both for τ^{electron} and τ^{hole}. In figure 6(b) the result is compared with experiment and the agreement is very good especially at small QW widths.

Results of figure 6 agree with the conclusion of [6] that the oscillatory behaviour of the experimental data implies the presence of the quantum electron capture (if the quantum electron capture were replaced by the classical one, agreement with experiment would be lost). However, the results of figure 6 show that the experiment indicates also

the presence of the quantum hole capture at least in the case of the narrowest (2.6 nm) QW sample, for which the classical hole capture is too slow (owing to $\ell_{\text{ph}} \gg w$) but the quantum hole capture model works well. For wider QWs the available experimental data support equally the quantum as well as classical hole capture models. For a definite conclusion a larger number of experimental data points would be desirable. For example, if the hole capture is of quantum nature, experiment should manifest a significant capture time enhancement at the QW width of ~3.4 nm and possibly also at the QW width of 6.2 nm (note the predicted maxima in figure 6(b)). On the other hand, if the hole capture is of classical nature, experiment should confirm that there are no other capture time maxima except for those already observed (19 ps at 2.6 nm, 15 ps at 7 nm).

Which of the two hole capture models can be justified theoretically? The Fermi golden rule based quantum capture model is expected [1, 2, 6] to fail if the carrier coherence length is smaller than the width of the AlGaAs/GaAs/AlGaAs region and such failure has indeed been quantitatively proven by means of a sophisticated theory beyond the Fermi golden rule [28]. Is the failure present also in our situation? Assume first that except for the optic phonon emission no other scattering process is operative. Since the carrier excitation energy is smaller than the optic phonon energy, the only possible scattering process is the transition into the energy state below the AlGaAs barrier, i.e. the carrier capture process. Thus the hole capture time represents directly the hole coherence time. If it is much longer than the time τ_{transit} necessary for the hole to overcome the distance between the AlAs sidewalls (~100 nm), then the hole should have time enough to create a standing-wave-like wavefunction and the quantum capture model should be justified. Indeed, if we take $\tau_{\text{transit}} \approx 2\tau_t$, where τ_t is given by equation (7), we obtain $\tau_{\text{transit}} \approx 3$ ps, which is mostly well below the capture time values in figures 4 and 6.

Can one ignore other coherence-breaking processes? The acoustic phonon scattering gives two orders longer time constants and can be neglected. Further, the measured capture times [6] are independent of the excitation density in the range 3×10^{15}–2×10^{17} cm^{-3}, which suggests that the carrier–carrier scattering effect is unimportant (it is a density dependent process). However, it is also possible that the carrier–carrier scattering breaks the hole coherence, but its density dependence [8] is not seen in the observed [6] capture time data due to the compensation by other density-dependent processes (screening of phonons, space charge). This issue needs a further investigation, which should rely on the 'non-golden-rule' quantum capture theory [28] in order to simulate the loss of the phase coherence and the corresponding transition between quantum (golden rule based) and classical (diffusion theory based) capture regimes.

Acknowledgment

Appendix. Carrier scattering rate within the DC phonon model

The treatment of the phonon confinement effect within the DC theory distinguishes the confined and interface phonon modes. We start with the discussion of the confined modes. The scattering effect of these modes can be treated in each of the layers of figure 1 separately, because the potential of the confined modes of each layer vanishes at the interfaces [13]. The carrier–polar optic phonon scattering rate due to the confined modes in the GaAs layer reads [15]

$$\lambda_{ij}(\varepsilon) = \frac{e^2 \omega_L}{2w} \left(\frac{1}{\kappa_\infty} - \frac{1}{\kappa_S} \right)$$
$$\times \sum_n \frac{|F_{ij}(n)|^2}{\left\{ \left[\left(\frac{n\pi}{w} \right)^2 \frac{\hbar^2}{2m} + E + \varepsilon \right]^2 - 4E\varepsilon \right\}^{1/2}} \quad \text{(A1)}$$

where

$$F_{ij}(n) = \int_{-w/2}^{w/2} dz \, \chi_i(z) \cos\left(\frac{n\pi}{w} z \right) \chi_j(z) \quad \text{(A2)}$$

for $n = 1, 3, 5, \dots$, and

$$F_{ij}(n) = \int_{-w/2}^{w/2} dz \, \chi_i(z) \sin\left(\frac{n\pi}{w} z \right) \chi_j(z) \quad \text{(A3)}$$

for $n = 2, 4, 6, \dots$. Other symbols are defined as in equation (1).

In the $Al_x Ga_{1-x} As$ layers the situation is more complicated owing to the presence of the GaAs-like and AlAs-like phonon branches [29], the phonon frequencies of which additionally depend on x [9]. In what follows we label the longitudinal and transversal phonon frequencies in the GaAs-like phonon branch as $\omega_{GL}(x)$ and $\omega_{GT}(x)$, respectively, and similarly we use $\omega_{AL}(x)$ and $\omega_{AT}(x)$ for the AlAs-like phonon branch. Let us consider the $Al_x Ga_{1-x} As$ layer on the right-hand side of the GaAs QW. In that layer, the confined modes of the phonon branch β ($\beta = $ GaAs, AlAs) give the scattering rate contribution

$$\lambda_{ij}^\beta(\varepsilon, x) = \frac{e^2}{b \kappa_\infty} \mathcal{C}_\beta(x)$$
$$\times \sum_n \frac{|F_{ij}(n)|^2}{\left\{ \left[\left(\frac{n\pi}{b} \right)^2 \frac{2\hbar^2}{m} + E_\beta + \varepsilon \right]^2 - 4E_\beta \varepsilon \right\}^{1/2}}$$
$$\beta = \text{GaAs, AlAs} \quad \text{(A4)}$$

where

$$F_{ij}(n) = \int_{\frac{w}{2}}^{\frac{w}{2} + \frac{b}{2}} dz \, \chi_i(z) \cos\left[\frac{n\pi}{b}(b + w - 2z) \right] \chi_j(z) \quad \text{(A5)}$$

for $n = 1, 3, 5, \dots$,

$$F_{ij}(n) = \int_{\frac{w}{2}}^{\frac{w}{2} + \frac{b}{2}} dz \, \chi_i(z) \sin\left[\frac{n\pi}{b}(b + w - 2z) \right] \chi_j(z) \quad \text{(A6)}$$

for $n = 2, 4, 6, \dots$,

$$\mathcal{C}_{\text{GaAs}}(x) = \omega_{GL}(x) \left[1 - \frac{\omega_{GT}^2(x)}{\omega_{GL}^2(x)} \right] \frac{\omega_{AT}^2(x) - \omega_{GL}^2(x)}{\omega_{AL}^2(x) - \omega_{GL}^2(x)} \quad \text{(A7)}$$

$$\mathcal{C}_{\text{AlAs}}(x) = \omega_{AL}(x) \left[1 - \frac{\omega_{AT}^2(x)}{\omega_{AL}^2(x)} \right] \frac{\omega_{AL}(x)^2 - \omega_{GT}^2(x)}{\omega_{AL}^2(x) - \omega_{GL}^2(x)} \quad \text{(A8)}$$

$E_{\text{GaAs}} = \varepsilon - E_j + E_i - \hbar\omega_{GL}(x)$, $E_{\text{AlAs}} = \varepsilon - E_j + E_i - \hbar\omega_{AL}(x)$ and the parameters κ_∞ and m are related [9] to the $Al_x Ga_{1-x} As$ material. (Derivation of the equations (A7) and (A8) can be found in [29].) Owing to the symmetry of the problem, equation (A4) holds also for the $Al_x Ga_{1-x} As$ layer on the left-hand side of the QW. Once the rates $\lambda_{ij}^{\text{GaAs}}(\varepsilon, x)$ and $\lambda_{ij}^{\text{AlAs}}(\varepsilon, x)$ are known, we obtain the resulting scattering rate $\lambda_{ij}^{\text{AlGaAs}}(\varepsilon, x)$ from the interpolation formula [15]

$$\lambda_{ij}^{\text{AlGaAs}}(\varepsilon, x) = (1 - x)\lambda_{ij}^{\text{GaAs}}(\varepsilon, x) + x\lambda_{ij}^{\text{AlAs}}(\varepsilon, x). \quad \text{(A9)}$$

Finally, the scattering by phonons in the AlAs layers can be ignored, because the wavefunction penetration into them is negligible.

Now we briefly summarize the theory of [30], which we use to calculate the scattering by interface modes. Unlike the confined modes, now the structure of figure 1 cannot be separated into three independent regions. The scattering rate due to the interface modes reads

$$\lambda_{ij}(\varepsilon) = \frac{e^2}{4\pi\hbar^2} \sum_m \sum_{l=s,a} \int_0^{2\pi} d\phi \left(\left[\frac{\partial}{\partial \omega} \kappa^W(\omega) \right] \right.$$
$$\left. - \frac{\kappa^W(\omega)}{\kappa^B(\omega)} \left[\frac{\partial}{\partial \omega} \kappa^B(\omega) \right] \right)^{-1} \left| \int_{-b/2}^{b/2} dz \, H_{ij}(l, \phi, z) \right|^2 \quad \text{(A10)}$$

where $\sum_m$ is the sum over all interface modes. The interface modes can be symmetric (s) and antisymmetric (a). The function H_{ij} is given as

$$H_{ij}(s, \phi, z) = \mathcal{P}^W \chi_i(z) \cosh[Q^W(\phi)z]\chi_j(z) \quad \text{(A11)}$$

$$H_{ij}(a, \phi, z) = \mathcal{P}^W \chi_i(z) \sinh[Q^W(\phi)z]\chi_j(z) \quad \text{(A12)}$$

$$\mathcal{P}^W = \sqrt{\frac{m^W}{Q^W(\phi) \sinh[Q^W(\phi)w]}} \quad \text{(A13)}$$

for $|z| \leqslant w/2$, and as

$$H_{ij}(s, \phi, z) = \mathcal{P}^B \chi_i(z) \sinh[Q^B(\phi)/2(z + w - 2|z|)]\chi_j(z) \quad \text{(A14)}$$

$$H_{ij}(a, \phi, z) = \mathcal{P}^B \chi_i(z) \, \text{sgn}(z)$$
$$\times \sinh[Q^B(\phi)/2(z + w - 2|z|)]\chi_j(z) \quad \text{(A15)}$$

$$\mathcal{P}^B = \sqrt{\frac{m^B \cosh[Q^B(\phi)w/2]}{Q^B(\phi) \sinh[Q^B(\phi)w] \sinh[Q^B(\phi)b/2]}} \quad \text{(A16)}$$

for $w/2 < |z| \leqslant b/2$.

Frequencies ω for the symmetric interface modes can be obtained from the equation

$$\kappa^W(\omega) \tanh[Q^\gamma(\phi)w/2] + \kappa^B(\omega) = 0 \quad \text{(A17)}$$

for the antisymmetric modes from the equation

$$\kappa^W(\omega) \coth[Q^\gamma(\phi)w/2] + \kappa^B(\omega) = 0 \quad \text{(A18)}$$

where γ is W for the QW region and B for the barrier regions. The wavevectors Q^γ are defined as

$$Q^\gamma(\phi) = \frac{\sqrt{2m^\gamma}}{\hbar}(\varepsilon + E - 2\sqrt{\varepsilon E}\cos\phi)^{1/2} \qquad (A19)$$

where $E = \varepsilon - E_j + E_i - \hbar\omega$, and the dielectric functions $\kappa^W(\omega)$ and $\kappa^B(\omega)$ as [30]

$$\kappa^W(\omega) = \kappa_\infty^W \frac{\omega^2 - (\omega_L)^2}{\omega^2 - (\omega_T)^2} \qquad (A20)$$

$$\kappa^B(\omega) = \kappa_\infty^B \frac{[\omega^2 - \omega_{AL}(x)^2][\omega^2 - \omega_{GL}(x)^2]}{[\omega^2 - \omega_{AT}(x)^2][\omega^2 - \omega_{AT}(x)^2]} \qquad (A21)$$

where ω_T is the transversal phonon frequency in the GaAs.

References

[1] Weller A, Thomas P, Feldmann J, Peter G and Göbel E O 1989 *Appl. Phys.* A **48** 509
[2] Grupen M and Hess K 1998 *IEEE J. Quantum Electron.* **34** 120
[3] Barros M R X, Becker P C, Morris S D, Deveaud B, Regreny A and Beisser F 1993 *Phys. Rev.* B **47** 10 951
[4] Fujiwara A, Takahashi Y, Fukatsu S, Shiraki Y and Ito R 1995 *Phys. Rev.* B **51** 2291
[5] Deveaud B, Chomette A, Morris D and Regreny A 1993 *Solid State Commun.* **85** 367
[6] Blom P W M, Smit C, Haverkort J E M and Wolter J H 1993 *Phys. Rev.* B **47** 2072
[7] Brum J A and Bastard G 1986 *Phys. Rev.* B **33** 1420
[8] Kálna K, Moško M and Peeters F M 1996 *Appl. Phys. Lett.* **68** 117
[9] Adachi S 1985 *J. Appl. Phys.* **58** R1
[10] Goodnick S M and Lugli P 1988 *Phys. Rev.* B **37** 2578
[11] Babiker M and Ridley B K 1986 *Superlatt. Microstruct.* **2** 287
[12] Ridley B K 1994 *Phys. Rev.* B **50** 1717
[13] Mori N and Ando T 1989 *Phys. Rev.* B **40** 6175
[14] Chen R, Lin D L and George T F 1990 *Phys. Rev.* B **41** 1435
[15] Rücker H, Molinari E and Lugli P 1992 *Phys. Rev.* B **45** 6747
[16] Lee I, Goodnick S M, Gulia M, Molinari E and Lugli P 1995 *Phys. Rev.* B **51** 7046
[17] Weber G and Paula A M 1993 *Appl. Phys. Lett.* **63** 3026
[18] Stavrou V N, Bennett C R, Babiker M, Zakhleniuk N A and Ridley B K 1998 *Phys. Low-Dimensional Struct.* **1/2** 23
[19] Dingle R, Wiegmann W and Henry C H 1974 *Phys. Rev. Lett.* **33** 827
[20] Weisbuch C and Vinter B 1991 *Quantum Semiconductor Structures: Fundamentals and Applications* (San Diego, CA: Academic) p 59
[21] Höpfel R A, Shah J and Juen S 1992 *Hot Carriers in Semiconductor Nanostructures* ed J Shah (San Diego, CA: Academic) p 379
[22] Hess K, Morkoç H, Shichijo H and Streetman B G 1979 *Appl. Phys. Lett.* **35** 469
[23] Nag B R 1980 *Electron Transport in Compound Semiconductors* (Heidelberg: Springer) p 119
[24] Reik H G and Risken H 1961 *Phys. Rev.* **124** 777
[25] Hohenester U, Supancic P, Kocevar P, Zhou X Q, Kütt W and Kurz H 1993 *Phys. Rev.* B **47** 13 233
[26] Landau L D and Lifshitz E M 1958 *Quantum Mechanics, Non-Relativistic Theory* 3rd edn (London: Pergamon) p 76
[27] Even if we accepted that μ_h is as low as 1440 cm^2 V^{-1} s^{-1} (say due to the hole–electron collisions), the actual classical capture time would still be given by equation (11), now with $\tau_t = 12.5$ ps. The resulting τ^{hole} would then be much larger than 12.5 ps and the fit of the experimental data would fail again.
[28] Register L F and Hess K 1995 *Superlatt. Microstruct.* **18** 223
[29] Swierkowski L, Zawadski W, Guldner Y and Rigaux C 1978 *Solid State Commun.* **27** 1245
[30] Kim K W and Stroscio M A 1990 *J. Appl. Phys.* **68** 6289